MOLECULAR AND CELLULAR BIOLOGY, Jan. 2010, p. 273–283 Vol. 30, No. 1
0270-7306/10/$12.00 doi:10.1128/MCB.01143-09

Impaired Lysosomal Trimming of N-Linked Oligosaccharides Leads to Hyperglycosylation of Native Lysosomal Proteins in Mice with α-Mannosidosis▽

Markus Damme,[1] Willy Morelle,[2] Bernhard Schmidt,[1] Claes Andersson,[3] Jens Fogh,[3] Jean-Claude Michalski,[2] and Torben Lübke[1]*

Abt. Biochemie II, Georg-August Universität Göttingen, Humboldtallee 23, 37073 Göttingen, Germany[1]; Unité Mixte de Recherche CNRS/USTL 8576, Glycobiologie Structurale et Fonctionelle, IFR 147, Bâtiment C9, Université des Sciences et Technologies de Lille 1, 59655 Villeneuve d'Ascq, France[2]; and Zymenex A/S, Roskildevej 12C, 3400 Hillerød, Denmark[3]

Received 24 August 2009/Returned for modification 21 September 2009/Accepted 21 October 2009

α-Mannosidosis is caused by the genetic defect of the lysosomal α-D-mannosidase (LAMAN), which is involved in the breakdown of free α-linked mannose-containing oligosaccharides originating from glycoproteins with N-linked glycans, and thus manifests itself in an extensive storage of mannose-containing oligosaccharides. Here we demonstrate in a model of mice with α-mannosidosis that native lysosomal proteins exhibit elongated N-linked oligosaccharides as shown by two-dimensional difference gel electrophoresis, deglycosylation assays, and mass spectrometry. The analysis of cathepsin B-derived oligosaccharides revealed a hypermannosylation of glycoproteins in mice with α-mannosidosis as indicated by the predominance of extended Man3GlcNAc2 oligosaccharides. Treatment with recombinant human α-mannosidase partially corrected the hyperglycosylation of lysosomal proteins in vivo and in vitro. These data clearly demonstrate that LAMAN is involved not only in the lysosomal catabolism of free oligosaccharides but also in the trimming of asparagine-linked oligosaccharides on native lysosomal proteins.

The lysosomal α-D-mannosidase (LAMAN; EC 3.2.1.24) belongs to the group of at least seven lysosomal exoglycosidases which sequentially degrade oligosaccharides derived from glycoproteins (2, 31). These glycoproteins enter the lysosomal compartment by either endocytic pathways (extracellular and plasma membrane proteins) or autophagic processes (intracellular proteins). In addition, free oligosaccharides originating from lipid-linked oligosaccharides in the endoplasmic reticulum and from glycoproteins by the endoplasmic reticulum-associated protein degradation (ERAD) pathway are transported into the lysosome, where these oligosaccharides are subsequently degraded (9, 45). Inside the lysosome, the degradation of the glycoproteins is described as a bidirectional process in which on the one hand the polypeptide is hydrolyzed by a cohort of lysosomal endo- and exoproteases with partially overlapping specificities like cathepsins and other peptidases (like DPP II and TPP-I [19, 40, 52). On the other hand, the sugar moiety is stepwise hydrolyzed into its monosaccharides by exoglycosidases. The precise order of the bidirectional breakdown of glycoproteins is unclear, although assumptions can be made based on the analysis of the storage products of the different glycoproteinoses (31). Therefore, it is assumed that an efficient degradation of the oligosaccharide chain is highly dependent on the cleavage of the protein-oligosaccharide linkage by the glycosylasparaginase (2, 31). In contrast, the proteolysis of the polypeptide backbone is mainly unaffected by intact oligosaccharide structures on the glycoproteins (1).

LAMAN has a broad substrate specificity, cleaving nonreducing terminal α1,2-, α1,3-, and α1,6-mannosyl linkages found in complex-type, hybrid-type, and high-mannose-type asparagine-linked glycans (30, 60). Additionally, a second lysosomal mannosidase (MAN2B2) specific for the core α1,6 branch was characterized and found to be dependent on the prior enzymatic activity of lysosomal glycosylasparaginase or chitobiase, releasing Man3GlcNAc2 and Man3GlcNAc oligosaccharides, respectively (21, 36). The cooperation of this novel core-specific α1,6-mannosidase with chitobiase is also reflected by their similar tissue-specific expression patterns in humans and rodents and their simultaneous absence in cattle and cats (2, 14).

LAMAN deficiency results in the rare lysosomal storage disorder (LSD) α-mannosidosis, which is clinically characterized by progressive mental retardation, dysostosis multiplex, impaired hearing, immune defects, and mild hepatosplenomegaly. However, the onset of symptoms varies greatly and the clinical severity of α-mannosidosis patients ranges from mildly affected to severely affected, lacking a genotype-phenotype correlation (29). Patients also show elevated serum and urine oligosaccharide levels and an enlargement of the lysosomal compartment which is considered to be caused by the accumulation of undegraded oligosaccharides. The major lysosomal storage product is the trisaccharide Man2GlcNAc, although oligosaccharides with up to eight mannosyl residues were detected in the urine and serum of patients, indicating their lysosomal accumulation as well (4, 33). From these findings, one can draw the conclusion that beside metabolic intermediates of the glycoprotein degradation, a considerable number of

* Corresponding author. Mailing address: Zentrum Biochemie und Molekulare Zellbiologie, Abteilung Biochemie II, Georg-August Universität Göttingen, Humboldtallee 23, 37073 Göttingen, Germany. Phone: 49-551-395932. Fax: 49-551-395979. E-mail: tluebke@gwdg.de.
▽ Published ahead of print on 2 November 2009.

oligosaccharides originate from dolichol-linked oligosaccharides or from glycoproteins that failed quality control in the endoplasmic reticulum and thus are degraded by the proteasome, leaving behind highly mannosylated glycans (23, 32, 41). It is assumed that 70% of the stored oligosaccharides derive from complex- and hybrid-type glycans, 10% derive from high-mannose-type glycans, and 20% derive from biosynthetic intermediates, e.g., lipid-linked oligosaccharides (61).

Naturally occurring animal models for α-mannosidosis have been described for cats (8, 55), cattle (6, 24), and guinea pigs (12). The animal models have been the subjects of various studies dealing with neuropathological, behavioral, and therapeutic aspects of α-mannosidosis (3, 13, 38). It was shown with guinea pigs and cats that enzyme replacement therapy (ERT) and bone marrow transplantation, respectively, provided a benefit concerning clinical manifestations and remarkable success in the central nervous system of cats after bone marrow transplantation (13, 56).

Aside from the naturally occurring models, a mouse model for α-mannosidosis was generated in which the LAMAN gene was disrupted by gene targeting. This mouse model phenotypically resembled a mild variant of the human disease (46). We exploited this mouse model to develop an ERT approach as already clinically established for other LSDs like Gaucher disease, Hunter disease, or Pompe disease. For this purpose, LAMAN preparations from different species were proven to be efficacious for visceral organs, and most remarkably, we demonstrated that high-dose administration of recombinant human LAMAN (rhLAMAN) affected the central neural storage (39). Very recently, Blanz et al. confirmed the influence of high-dosage ERT on the peripheral as well as the central nervous system in the same mouse model and showed clearance of storage material in hippocampal neurons in particular (5). Here, we report on structural alterations of lysosomal proteins in mice with α-mannosidosis due to hyperglycosylation and the reversibility by ERT.

MATERIALS AND METHODS

Mice and ERT. Mice with α-mannosidosis and wild-type mice (C57BL/6 background) were used throughout the study (46). Animals were maintained under standard housing conditions on a 12-hour-light and 12-hour-dark schedule. All experiments were approved by local authorities (reference number G 46.04, Bezirksregierung Braunschweig). Experiments were done with 2- to 6-month-old animals.

For rhLAMAN treatment, mice were intravenously injected in the tail vein four times in 2 weeks with 100 mU/g body weight rhLAMAN (stock solution, 44 U/ml) in a total volume of 100 μl and sacrificed 2 days after the last injection. To control the amount of enzyme administered, blood was taken from the retroorbital plexus 5 minutes after injection. Storage of oligosaccharides was monitored by thin-layer chromatography as described previously (39).

Lysosome isolation (tritosomes). Mice were treated with a single injection of 0.75 mg tyloxapol (Triton WR1339; Sigma)/g body weight 4 days prior to liver removal. The isolation of tritosomes from tyloxapol-treated and control mice included differential centrifugation and isopycnic centrifugation and resulted in a lysosome-enriched fraction, F2, as described before (15, 58).

2-D gel electrophoresis. For preparative two-dimensional (2-D) gel electrophoresis, 300 μg of lysosomal F2 fraction was acetone precipitated and resuspended in 100 μl lysis buffer {7 M urea, 2 M thiourea, 2% 3-[(3-cholamidylpropyl)-dimethylammonio]-1-propanesulfonate [CHAPS]}. One volume of rehydration buffer (lysis buffer with 2% [wt/vol] dithiothreitol [DTT], 2% immobilized pH gradient [IPG] buffer pH 4 to 7 [GE Healthcare]) was added, and samples were subsequently applied to IPG strips by rehydration overnight.

Isoelectric focusing (IEF) was performed according to standard protocols using IPG strips in the range of pH 4 to 7 (GE Healthcare, Munich, Germany) on an IPGPhor II unit (GE Healthcare). After calibration with DTT (10 mg/ml)- and iodacetamide (25 mg/ml)-containing equilibration buffer (6 M urea, 75 mM Tris-HCl, pH 8.8, 30% glycerol, 2% sodium dodecyl sulfate [SDS]), SDS-polyacrylamide gel electrophoresis (PAGE) was carried out on 15% gels made in-house. Preparative gels were stained with colloidal Coomassie brilliant blue G solution (Roth, Karlsruhe, Germany).

2-D fluorescence DIGE. CyDye difference gel electrophoresis (DIGE) Fluor minimal dyes (GE Healthcare, Munich, Germany) were used for fluorescence labeling. Twenty-five micrograms of F2 fractions in 10 μl lysis buffer (see above) derived from wild-type mice and mice with α-mannosidosis was labeled with 1 μl Cy3/Cy5 working solution (400 pmol/μl in dimethyl formamide), respectively, for 30 min on ice in the dark. The labeling reaction was quenched by the addition of 1 μl of 10 mM lysine. After addition of 90 μl lysis buffer, 2-D electrophoresis was performed as described above. Fluorescence was scanned with the appropriate wavelengths for Cy3 and Cy5 with a Typhoon 9400 scanner (GE Healthcare).

Western blot analysis and antibodies. SDS-PAGE, Western blotting, and Coomassie blue staining were performed according to standard protocols. The following antibodies and antisera were used for immunoblotting: anti-cathepsin B (Neuromics), anti-cathepsin E (personal gift from Y. Ohsumi [unpublished data]), anti-NPC2 protein (rabbit antibody against recombinant human NPC2; gift of Shutish Patel; see also reference 59), anti-Scpep1 (25), and anti-glyceraldehyde-3-phosphate dehydrogenase (anti-GAPDH; FL-335; Santa Cruz).

Lectin Western blotting. Twenty-five micrograms of F2 fractions was separated by 15% SDS-PAGE and subsequently blotted on a polyvinylidene difluoride (PVDF) membrane. Membranes were incubated with biotin-conjugated *Lens culinaris* lectin (2 μg/μl; Vector Laboratories, Burlingame, CA) in 3% bovine serum albumin overnight and detected with horseradish peroxidase-conjugated streptavidin. No streptavidin-cross-reacting bands were observed when the *Lens culinaris* lectin was omitted.

Deglycosylation experiments. Thirty micrograms of lysosomal fractions was subjected to rhLAMAN, peptide *N*-glycosidase F (PNGase F), and endoglycosidase H (Endo H) treatment. LAMAN treatment was performed under native lysosomal conditions in 100 mM citrate buffer (pH 4.6) and 1 mM phenylmethylsulfonyl fluoride with 200 mU of rhLAMAN for 16 h at 37°C. PNGase F and Endo H treatments were performed as recommended by the manufacturer (Roche).

In-gel PNGase F digestion. The Coomassie blue-stained bands were excised from the gel by using a scalpel and transferred into microcentrifuge tubes. Each excised gel piece was further destained by being washed several times with the two following solutions: 50 mM ammonium bicarbonate acetonitrile (1:1, vol/vol) and acetonitrile for 20 min. The solution was then removed, and the gel pieces were dehydrated with acetonitrile for 20 min. After acetonitrile was removed, the gel pieces were left to dry in a vacuum centrifuge for 30 min at room temperature. Each gel piece was further suspended in 50 mM ammonium bicarbonate containing 20 mM DTT. Bands corresponding to peptides were then reduced at 56°C for 45 min. After the DTT-containing supernatant was removed, each gel piece was suspended with 50 mM ammonium bicarbonate containing 110 mM of iodoacetamide (IAA) and S alkylation was conducted overnight in the dark at room temperature. The alkylating reagent-containing solution was removed, and the gel pieces were washed several times in 100 mM ammonium bicarbonate for 20 min. The gel pieces were finally dehydrated with acetonitrile and dried in the vacuum centrifuge for 45 min.

The dried gel pieces were rehydrated in 20 mM ammonium bicarbonate buffer (pH 8.3) containing 1 U of PNGase F, and enzymatic deglycosylation was performed at 37°C overnight. The PNGase F-released N-glycans were eluted from the gel pieces with water three times for 20 min. The pooled extracted glycans were dried in a vacuum centrifuge and then desalted on minicolumns with 10 mg of nonporous graphitized carbon. The columns were sequentially washed with 1 ml of methanol and 2 ml of 0.1% (vol/vol) trifluoroacetic acid (TFA). The glycans were dissolved in 300 μl of 0.1% (vol/vol) TFA, applied to the column, and washed with 2 ml of 0.1% (vol/vol) TFA. The elution of glycans was conducted with the application of 1 ml of 25% (vol/vol) acetonitrile in water containing 0.1% (vol/vol) TFA. The fractions were dried in a vacuum centrifuge.

MALDI mass spectrometry. Matrix-assisted laser desorption ionization (MALDI) mass spectrometry experiments for oligosaccharide analysis were carried out on a Voyager Elite DE-STR Pro instrument (PerSeptive Biosystems, Framingham, MA) equipped with a pulsed nitrogen laser (337 nm) and a gridless delayed-extraction ion source. The spectrometer was operated in positive reflectron mode by delayed extraction with an accelerating voltage of 20 kV, a pulse delay time of 200 ns, and a grid voltage of 66%. All spectra shown represent accumulated spectra obtained by 400 to 500 laser shots. The sample was prepared by mixing a 1-μl aliquot (5 to 10 pmol) with 1 μl of matrix solution on the

MALDI sample plate. The matrix solution was prepared by saturating methanol-water (1:1) with 2,5-dihydroxybenzoic acid (10 mg/ml). Peptide mass fingerprint (PMF) analysis was performed as described by Kollmann et al. (26) on a Reflex III MALDI-time of flight (TOF) mass spectrometer (Bruker Daltonik, Bremen, Germany).

RESULTS

Isolation and identification of lysosomal proteins from mouse liver. To obtain lysosome-enriched fractions (F2) from mouse liver, mice were treated with tyloxapol 4 days prior to liver removal. Tyloxapol inhibits the lipoprotein lipase and causes an increased endocytosis and delivery of low-density lipoprotein into the lysosomes of the hepatocytes. Hence, the density of the lysosomes is selectively altered so that they can be efficiently separated from other organelles. Three livers of either control mice or mice with α-mannosidosis were pooled and subsequently subjected to differential centrifugation and a single discontinuous sucrose density gradient. The resulting lysosome-enriched fraction is 40- to 50-fold enriched in lysosomal marker proteins like β-hexosaminidase or α-glucuronidase (data not shown). We tested the quality of the lysosomal preparation by 2-D gel electrophoresis followed by mass spectrometry analysis. Therefore, 300 μg of protein of lysosome-enriched fraction F2 from control mice was separated on a conventional 2-D gel, visualized by Coomassie blue staining, and analyzed by PMF assay. Figure 1 shows a representative 2-D map of the lysosome-enriched fraction F2 derived from three mice. We excised and analyzed a moderate number of 46 clearly separated protein spots and identified 17 lysosomal proteins in 43 protein spots. Two spots originated from non-lysosomal proteins, subunit d of the ATP synthase in spot 23 and the Cu/Zn superoxide dismutase in spot 32, and a third protein spot could not be identified (spot 34) (Fig. 1B). While some lysosomal proteins like the palmitoyl protein thioesterase 2 and arylsulfatase B were detected in a single spot, some lysosomal proteins were identified in a series of spots, e.g., cathepsin B (spots 7 to 13) or cathepsin D (spots 15 to 17, 24 to 28, 40, and 41), due to heterogeneity in size and charge that is caused posttranslationally by processes like limited proteolysis and trimming of N-linked oligosaccharides. These results confirm that the F2 fraction from mouse liver preferentially consists of soluble lysosomal proteins.

2-D DIGE analysis of mouse liver lysosomal proteins. In order to reveal differences in the protein compositions of the lysosomal compartments from control mice and mice with α-mannosidosis, lysosome-enriched fraction F2 was analyzed by 2-D fluorescence DIGE analysis. Equal amounts of proteins (25 μg) from fraction F2 of three control mice and of three mice with α-mannosidosis were labeled with Cy3 and Cy5, respectively. The samples were combined and subjected to IEF using a pH gradient ranging from pH 4 to 7 in the first dimension and a 15% SDS-polyacrylamide gel in the second dimension. Proteins were visualized by in-gel fluorescent scanning.

Figure 2 shows the overlay picture of the Cy3-labeled control sample and the Cy5-labeled α-mannosidosis sample. Remarkably, most proteins of the mixture appeared as two single spots that merged vertically into each other rather than as yellow single spots as a result of a merge of Cy3- and Cy5-labeled protein populations. In particular, proteins with an apparent molecular mass of less than 50 kDa showed a tricolor-like appearance where Cy5-labeled lysosomal proteins derived from mice with α-mannosidosis presented exclusively with higher molecular weights than those of the Cy3-labeled proteins from control mice, with partial yellow overlay in between. The shift of a large portion of lysosomal proteins from the mice with α-mannosidosis toward higher molecular weights, however, hampered the quantitative analysis of lysosomal proteins in the α-mannosidosis murine model by the 2-D DIGE approach.

Detection of abnormally glycosylated proteins in a lysosome-enriched fraction from the liver of a mouse with α-mannosidosis. One common hallmark of lysosomal proteins is their extensive glycosylation. The shift in the molecular weight of lysosomal proteins from mice with α-mannosidosis could be due to an altered glycosylation pattern. To test this hypothesis, lysosome-enriched fractions from control mice and mice with α-mannosidosis were analyzed for glycoproteins with terminal α-D-mannosyl and α-D-glucosyl residues using biotinylated *Lens culinaris* lectin after separation by SDS-PAGE and transfer on a PVDF membrane. As shown in Fig. 3, *Lens culinaris* lectin detected significantly larger amounts of distinct glycoproteins in F2 fractions of mice with α-mannosidosis (lanes 4 to 6) than in F2 fractions from control mice (lanes 1 to 3). In particular, a number of strong signals exclusively emerged in F2 samples from mice with α-mannosidosis with apparent molecular masses of 50 kDa, 40 kDa, 32 kDa, and 28 kDa. Most likely, the 32-kDa and 28-kDa samples represent cathepsin B forms corresponding to spots 7 to 10 and 11 and 12 in the 2-D gel (Fig. 1). From these results we concluded that at least some lysosomal glycoproteins of mice with α-mannosidosis show altered glycosylation patterns.

Hyperglycosylation of lysosomal proteins in mice with α-mannosidosis is corrected by ERT. To reveal whether the molecular weight shift is ascribed to the altered N-glycans of lysosomal proteins in mice with α-mannosidosis, we analyzed liver homogenates by PNGase F treatment followed by SDS-PAGE and detection of the lysosomal proteins cathepsin B (Fig. 4A, top panel) and NPC2 protein (Fig. 4A, middle panel). In order to demonstrate that the molecular weight shift of the lysosomal proteins is a result of the α-mannosidase deficiency, we treated the mice with α-mannosidosis for 2 weeks with four injections, applying 100 mU/g body weight rhLAMAN prior to organ removal (39). The efficiency of the ERT was controlled by analyzing the storage of neutral oligosaccharides as described before (39 and data not shown).

The lysosomal active forms of cathepsin B are represented by a 30-kDa single-chain (SC) form and a double-chain form consisting of a disulfide-linked 5-kDa N-terminal fragment and a 24-kDa C-terminal fragment (28) containing two putative N-glycosylation sites (N192 and N208). PNGase F treatment only slightly altered the apparent sizes of both lysosomal cathepsin B forms (30 kDa and 24 kDa) in control mice (Fig. 4A, top panel, lanes 1 and 2). In contrast, lysosomal cathepsin B from mice with α-mannosidosis showed significantly higher apparent sizes, with 32 kDa for the SC form and 28 kDa for the double-chain form (lane 3), and could be normalized by PNGase F treatment toward the wild-type forms (lane 4). ERT corrected the size increase observed for mature cathepsin B forms in mice with α-mannosidosis to normal (32-kDa SC form) or nearly normal (24-kDa form, lane 5). PNGase F

A

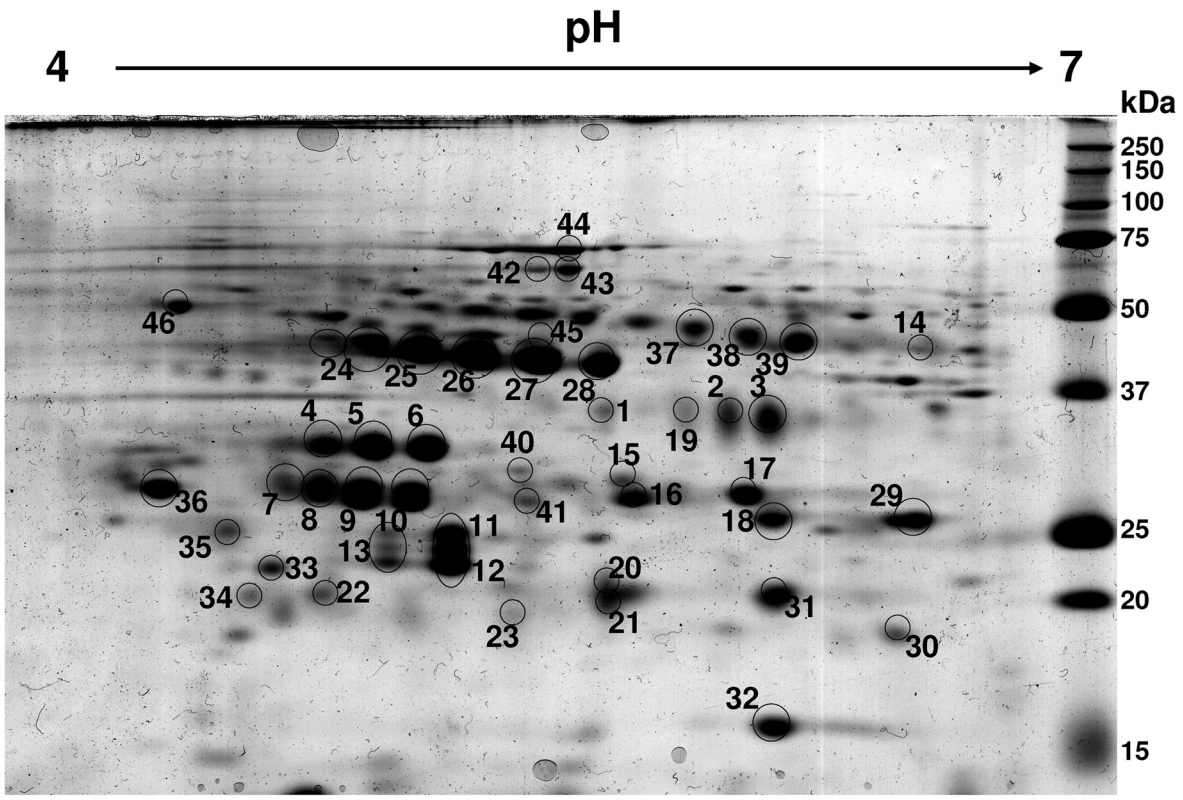

B

Protein analysis by peptide mass fingerprint – arbitrary selected spots from the 2-DE gel (see upper panel) of a lysosome-enriched fraction F2-fraction; * Mowse scores > 64 are significant ($p < 0.05$)

No.	protein	predicted molecular mass (Dalton)	*gene accession-* No.	Mowse-Score *
1	palmitoyl-protein thioesterase 2 (PPT2)	34686	gi|9506985	71
2	legumain	49740	gi|7242487	156
3	legumain	49740	gi|7242487	267
4	cathepsin Z	34837	gi|11968166	175
5	cathepsin Z	34837	gi|11968166	255
6	cathepsin Z	34837	gi|11968166	275
7	cathepsin B	38282	gi|6681079	155
8	cathepsin B	38282	gi|6681079	282
9	cathepsin B	38282	gi|6681079	272
10	cathepsin B	38282	gi|6681079	390
11	cathepsin B	38282	gi|6681079	172
12	cathepsin B	38282	gi|6681079	141
13	cathepsin B	38282	gi|6681079	155
14	arylsulfatase B	63012	gi|148668607	196
15	cathepsin D	45381	gi|74220823	64
16	cathepsin D	45381	gi|74220823	73
17	cathepsin D	45381	gi|74220823	162
18	cathepsin H	37701	gi1705636	77
19	legumain	34837	gi|7242487	82
20	cellular repressor of E1A-stimulated gene (CREG)	24550	gi|6753520	143
21	cellular repressor of E1A-stimulated gene (CREG)	24550	gi|6753520	135
22	cathepsin C	53141	gi|74199074	73
23	ATP-Synthase, subunit d	15929	gi|159572410	168
24	cathepsin D	45381	gi|74220823	123
25	cathepsin D	45381	gi|74220823	162
26	cathepsin D	45381	gi|74220823	155
27	cathepsin D	45381	gi|74220823	135
28	cathepsin D	45381	gi|74220823	74
29	cathepsin H	37701	gi|1705636	128
30	cathepsin A / protective protein	54437	gi|84042525	106
31	cathepsin H	37701	gi|3929819	105
32	Cu/Zn superoxide dismutase	16104	gi|226471	162
33	GM2-ganglioside activator protein	21267	gi|6806917	95
34	not identified	-	-	-
35	lysosomal thiol reductase	28535	gi|11345388	38
36	cathepsin A /protective protein	54437	gi|84042523	86
37	tripeptidyl-peptidase I (TPP1)	59067	gi|3766471	63
38	tripeptidyl-peptidase I (TPP1)	59067	gi|3766471	67
39	tripeptidyl-peptidase I (TPP1)	59067	gi|3766471	54
40	cathepsin D	45381	gi|6753556	182
41	cathepsin D	45381	gi|6753556	182
42	lysosomal α-glucosidase	106921	gi|51338793	162
43	lysosomal α-glucosidase	106921	gi|51338793	180
44	albumin	70700	gi|26342396	366
45	di-N-acetyl-chitobiase	35912	gi|67460414	224
46	dipeptidyl-peptidase 2	56804	gi|13626390	169

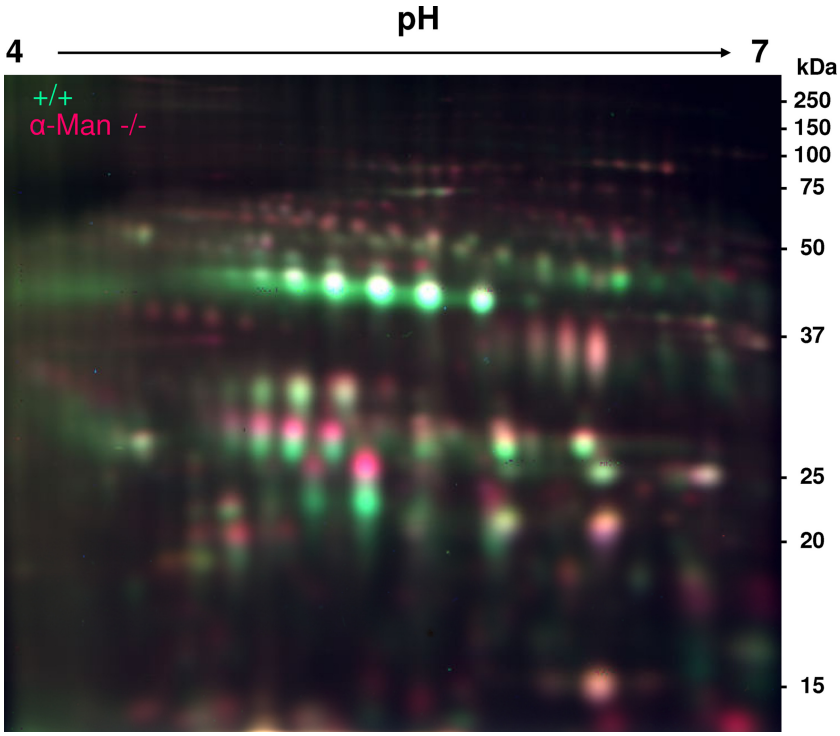

FIG. 2. 2-D DIGE analysis of lysosome-enriched fractions (F2) from wild-type mice and mice with α-mannosidosis. Twenty-five micrograms of protein of an F2 fraction from wild-type mice was labeled with Cy3 (green), and 25 μg of protein of an F2 fraction from mice with α-mannosidosis was labeled with Cy5 (red). The labeled protein fractions were mixed, separated as described above by 2-D gel electrophoresis, and finally analyzed by fluorescence scanning. The merge picture shows that Cy5-labeled lysosomal proteins derived from the mice with α-mannosidosis generally exhibited higher molecular masses than those of their Cy3-labeled counterparts from wild-type mice, indicating an impaired processing or altered glycosylation of lysosomal proteins in mice with α-mannosidosis.

treatment of the homogenates from ERT-treated mice with α-mannosidosis finally resulted in the normalization of the cathepsin B double-chain form (lane 6). NPC2 protein from livers of wild-type mice mainly occurred with an apparent molecular size of 15 kDa (Fig. 4A, middle panel, lane 1), while in mice with α-mannosidosis it was detected at 18 kDa (lane 3). Both genotypes also exhibited a faint signal for NPC2 protein at 16 kDa. The deglycosylation of NPC2 protein of whatever origin—wild-type mice, mice with α-mannosidosis, or mice with α-mannosidosis after ERT—resulted in single signals of 14 kDa in apparent size (lanes 2, 4, and 6). ERT corrected the increased size of the NPC2 protein, partially resulting in a 17-kDa intermediate (lane 5). Similar observations were made for cathepsin E and the novel lysosomal protein Scpep1 (25) (data not shown). In summary, the deglycosylation analysis demonstrates that a number of lysosomal proteins are hyperglycosylated in mice with α-mannosidosis and that the glycosylation can be partially normalized in vivo by ERT.

Endo H selectively removes high-mannose-type and hybrid-type glycans consisting of at least four mannose residues from glycoproteins. We incubated liver homogenates from wild-type mice, mice with α-mannosidosis, or ERT-treated mice with α-mannosidosis with or without Endo H and assayed for cathepsin B (Fig. 4B, top panel) and NPC2 protein (Fig. 4B, middle panel). Cathepsin B from wild-type mice and mice with α-mannosidosis as well as ERT-treated mice with α-mannosidosis was resistant to Endo H treatment, indicating that the molecular shift must be due to N-glycans from complex-type or partially trimmed core glycans with fewer than four mannose residues (Fig. 4B, top panel). In wild-type mice, NPC2 protein was also resistant to Endo H treatment (Fig. 4B, middle panel, lanes 1 and 2). In contrast, NPC2 protein from

FIG. 1. (A) 2-D gel electrophoresis map of proteins from a lysosome-enriched fraction (F2) derived from mouse liver after subcellular fractionation. Three hundred micrograms of protein of an F2 fraction from wild-type mice was separated by IEF (pH gradient 4 to 7) in the first dimension followed by SDS-PAGE on a 15% gel in the second dimension. The gel was stained with Coomassie blue, and the arbitrarily numbered protein spots (black circles) were excised and analyzed by PMF assay. A total of 46 protein spots were identified, of which 43 spots represented 17 lysosomal proteins while two spots—spot 23 and spot 32—contained the mitochondrial proteins ATP-synthase subunit d and Cu/Zn superoxide dismutase, respectively (see also panel B). One protein spot could not be identified (spot 34). For example, the lysosomal protein cathepsin B was identified in a series of protein spots (spots 7 to 13) with different isoelectric points and different apparent molecular masses. (B) Proteins identified by PMF according to the arbitrary numbering in the 2-D gel (A). We also itemized the predicted molecular mass, the gene accession number, and the Mowse score for each identified protein.

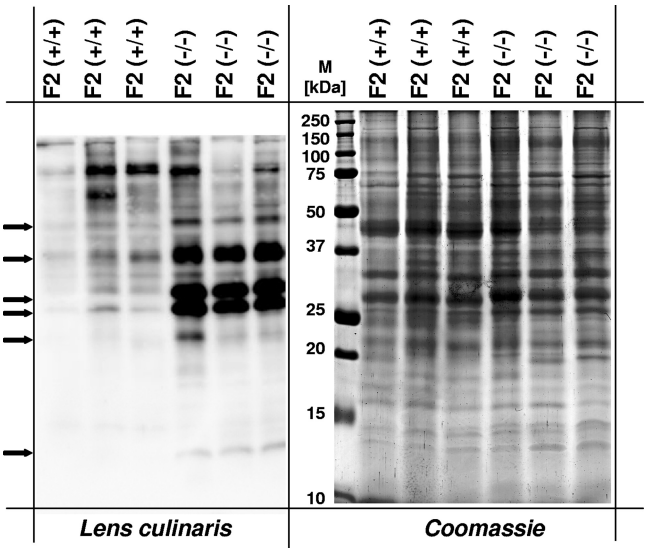

FIG. 3. *Lens culinaris* lectin blotting of lysosome-enriched fractions (F2) from wild-type mice and mice with α-mannosidosis. Thirty micrograms of F2 fractions from three wild-type mice and three mice with α-mannosidosis was separated by SDS-PAGE and blotted on a PVDF membrane. Glycoproteins were detected by biotinylated *Lens culinaris* lectin and horseradish peroxidase-coupled streptavidin (left panel). For a loading control, a duplicate gel was stained with Coomassie blue (right panel). Arrows indicate glycoproteins with differences in *Lens culinaris* reactivity.

mice with α-mannosidosis showed a clear reduction in apparent molecular weight upon Endo H treatment (Fig. 4B, middle panel, lanes 3 and 4) while in ERT-treated mice with α-mannosidosis a wild-type-like deglycosylation pattern was observed (middle panel, lane 6), indicating that NPC2 protein of mice with α-mannosidosis possesses high-mannose-type or hybrid-type glycans while NPC2 protein from wild-type mice exhibits N-glycans with fewer than four mannosyl residues.

The hyperglycosylation of lysosomal proteins is apparent in all tested tissues of mice with α-mannosidosis. In order to reveal whether the hyperglycosylation of lysosomal proteins in mice with α-mannosidosis is restricted to the liver or also holds true for other tissues and for the brain in particular, we analyzed various tissues from mice with α-mannosidosis and wild-type mice regarding the apparent molecular size of cathepsin B and NPC2 protein by Western blot analysis (Fig. 4C). In all tested tissues, cathepsin B (Fig. 4C, top panel) and NPC2 protein (middle panel) from mice with α-mannosidosis showed increased apparent molecular sizes, indicating that the hyperglycosylation of lysosomal proteins is a general hallmark of α-mannosidosis-affected tissues rather than a liver-specific characteristic. Moreover, the relative amount of some tested lysosomal proteins like NPC2 protein was markedly elevated in tissues from mice with α-mannosidosis (Fig. 4C).

Differences in the N-glycan structures of cathepsin B from control mice and mice with α-mannosidosis. To further characterize the abnormal molecular forms of cathepsin B and their glycans from mice with α-mannosidosis, we analyzed cathepsin B from F2 fractions of control mice and mice with α-mannosidosis by conventional 2-D gel electrophoresis and subsequent Coomassie blue staining (Fig. 5A). Cathepsin B from control mice was identified by mass spectrometry in 10 spots ranging from pH 5 to pH 5.8 and apparent molecular sizes ranging from 24 kDa to 32 kDa (Fig. 5A, left panel). Interestingly, cathepsin B from control mice was arranged in four double spots of 32 kDa and 30 kDa, respectively, in size and isoelectric points (pIs) of 5 to 5.6 and three spots with an isoelectric point of 5.8 and apparent molecular sizes of 24, 26, and 28 kDa representing the large chain of the double-chain form. In contrast, cathepsin B from mice with α-mannosidosis (Fig. 5A, right panel) was identified in only four single spots of 32 kDa and one prominent spot for the large chain of the double-chain form with an apparent size of 28 kDa and a minor spot of 24 kDa. Regarding their isoelectric points, cathepsin B proteins from control mice and from mice with α-mannosidosis showed comparable distributions.

We excised the cathepsin B spots from the gel, released the N-glycans by PNGase F treatment, and pooled the N-glycans from the appropriate genotypes prior to a semiquantitative analysis by MALDI-TOF mass spectrometry. Thereby, it became obvious that N-glycans from wild-type mice consisted mainly of the Man2GlcNAc2 and the core fucosylated Man2GlcNAc2 forms (Fig. 5B, upper panel). Larger oligosaccharides (Man3GlcNAc2, fucosylated Man3GlcNAc2, and Man4GlcNAc2) were present only in trace amounts. In contrast, the major glycans from cathepsin B of the mice with α-mannosidosis were the Man3GlcNAc2 and the core fucosylated Man3GlcNAc2 forms, followed by the Man2GlcNAc2 forms and the Man4GlcNAc2 oligosaccharide—but also longer oligosaccharides like the Man7GlcNAc2 form were detectable. We also analyzed the N-linked oligosaccharides of each individual spot of the cathepsin B double-chain forms in wild-type mice and mice with α-mannosidosis and particularly detected extended oligosaccharides (Man3GlcNAc2 and fucosylated Man3GlcNAc2 as well as Man4-Man6GlcNAc2) in the 28-kDa form of double-chain cathepsin B from mice with α-mannosidosis (data not shown). In summary, cathepsin B from control mice and mice with α-mannosidosis contained mainly core oligosaccharides with two mannose residues and three mannose residues or even high-mannose glycans, respectively, suggesting that the trimming of polymannose glycans as well as the α1,3-linked core mannose is impaired in mice with α-mannosidosis.

α-Mannosidase is involved in N-glycan trimming of lysosomal proteins. Obviously, the hyperglycosylation of lysosomal proteins is a common hallmark of mice with α-mannosidosis, indicating that lysosomal α-mannosidase is involved in trimming of the N-linked oligosaccharides of lysosomal proteins within the lysosome. To demonstrate the ability of lysosomal α-mannosidase to trim N-glycans on native lysosomal proteins, we incubated protein of F2 fractions from wild-type mice and mice with α-mannosidosis in the presence or absence of 200 mU of rhLAMAN at pH 4.6 and examined NPC2 protein and cathepsin B for a size shift by immunoblotting. Figure 6A shows that in vitro NPC2 protein from control mice (lanes 1 and 2) was not altered in its apparent molecular size (15 kDa) after rhLAMAN incubation. In contrast, hyperglycosylated NPC2 protein with an apparent size of 18 kDa from mice with α-mannosidosis is reduced by rhLAMAN treatment to a molecular size that is comparable with that of NPC2 protein from control mice (lanes 5 and 6). To exclude the chance that the

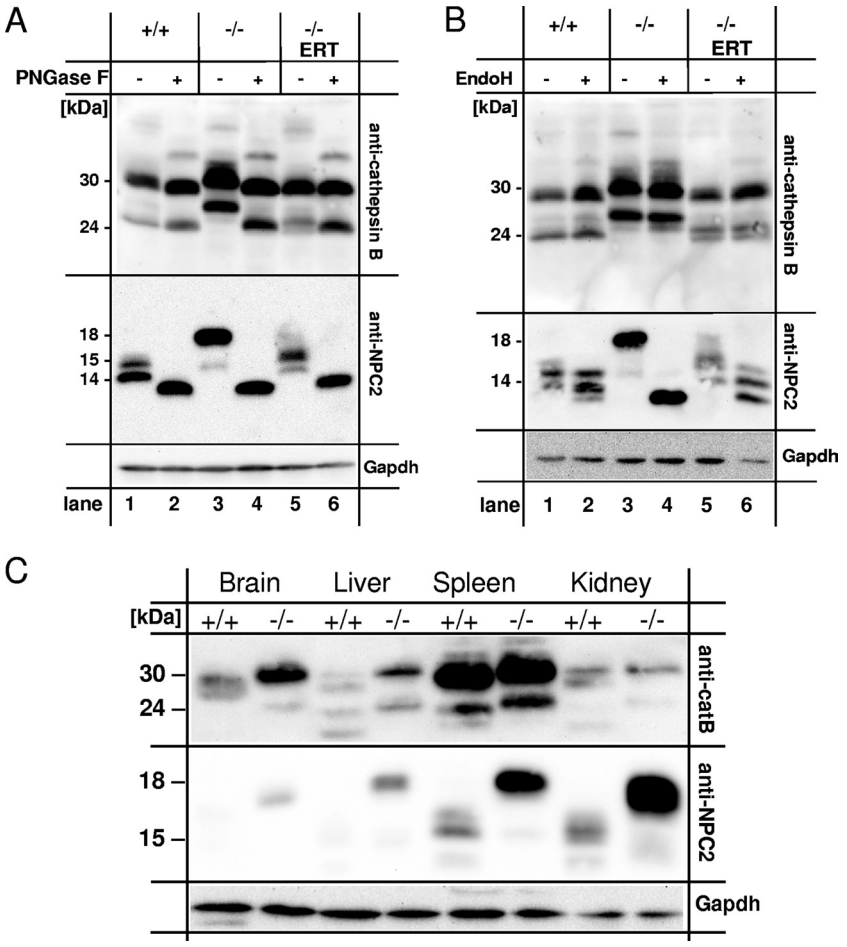

FIG. 4. (A and B) N glycosylation of lysosomal proteins in mouse liver homogenates from wild-type mice (+/+), mice with α-mannosidosis (−/−), and mice with α-mannosidosis after ERT (−/− ERT). One hundred micrograms of protein of mouse liver homogenates was incubated in the absence (−) or presence (+) of PNGase F (A) or Endo H (B), separated by SDS-PAGE, and subjected to immunoblotting using an anti-cathepsin B antibody (top panel) and an anti-NPC2 protein antibody (middle panel). GAPDH was detected as a loading control (bottom panel). (C) Multitissue Western blot analysis for cathepsin B and NPC2 protein. One hundred micrograms of total protein from various tissue homogenates from wild-type mice (+/+) and mice with α-mannosidosis mice (−/−) was separated by SDS-PAGE and assayed for cathepsin B (top panel), NPC2 protein (middle panel), and GAPDH as a loading control (bottom panel). Both lysosomal proteins, cathepsin B and NPC2 protein, exhibit higher molecular masses in tissues derived from mice with α-mannosidosis than in those from wild-type mice.

shift in the molecular weight of NPC2 protein from mice with α-mannosidosis results from residual proteolytic activity in the rhLAMAN preparation, we incubated the F2 either with PNGase F (Fig. 6, lanes 3 and 7) alone or sequentially with rhLAMAN and PNGase F (Fig. 6, lanes 4 and 8). PNGase F deglycosylation of NPC2 protein—regardless of genotype or rhLAMAN pretreatment—always resulted in the expected signal of 14 kDa as demonstrated before (also Fig. 4). The same proved true for the hyperglycosylated cathepsin B (Fig. 6B) and Scpep1 (data not shown) from mice with α-mannosidosis.

DISCUSSION

There is in-depth knowledge of the processes during the biogenesis of lysosomal glycoproteins until their enzymatic activation including N glycosylation, limited proteolysis, and mannose 6-phosphate labeling, whereas little is known about their fate and mode of breakdown inside the lysosome. So far, it has been demonstrated that the mannose 6-phosphate signal is removed in a prelysosomal compartment (17) and the lysosome (7) with tissue- and environment-dependent dephosphorylation kinetics (16, 44). Recently, it was proposed that acid phosphatase 5 (Acp5) is critical for the dephosphorylation of the 6-phosphomannosyl residue (47).

Here, we show that many lysosomal soluble glycoproteins undergo an extensive trimming process on their N-linked oligosaccharides inside the lysosome that is dependent on α-D-mannosidase activity. Our DIGE analysis revealed that in mice with α-mannosidosis numerous lysosomal soluble proteins exhibit increased apparent molecular weights compared to the same set of proteins from control mice. Such an increase in molecular size could be assigned to either incomplete limited proteolysis or a hyperglycosylation of the lysosomal proteins. By PNGase F treatment we could demonstrate for various lysosomal soluble proteins like cathepsin B, NPC2 protein, cathepsin E, and Scpep1 that hyperglycosylation causes the molecular shift in mice with α-mannosidosis and that this hy-

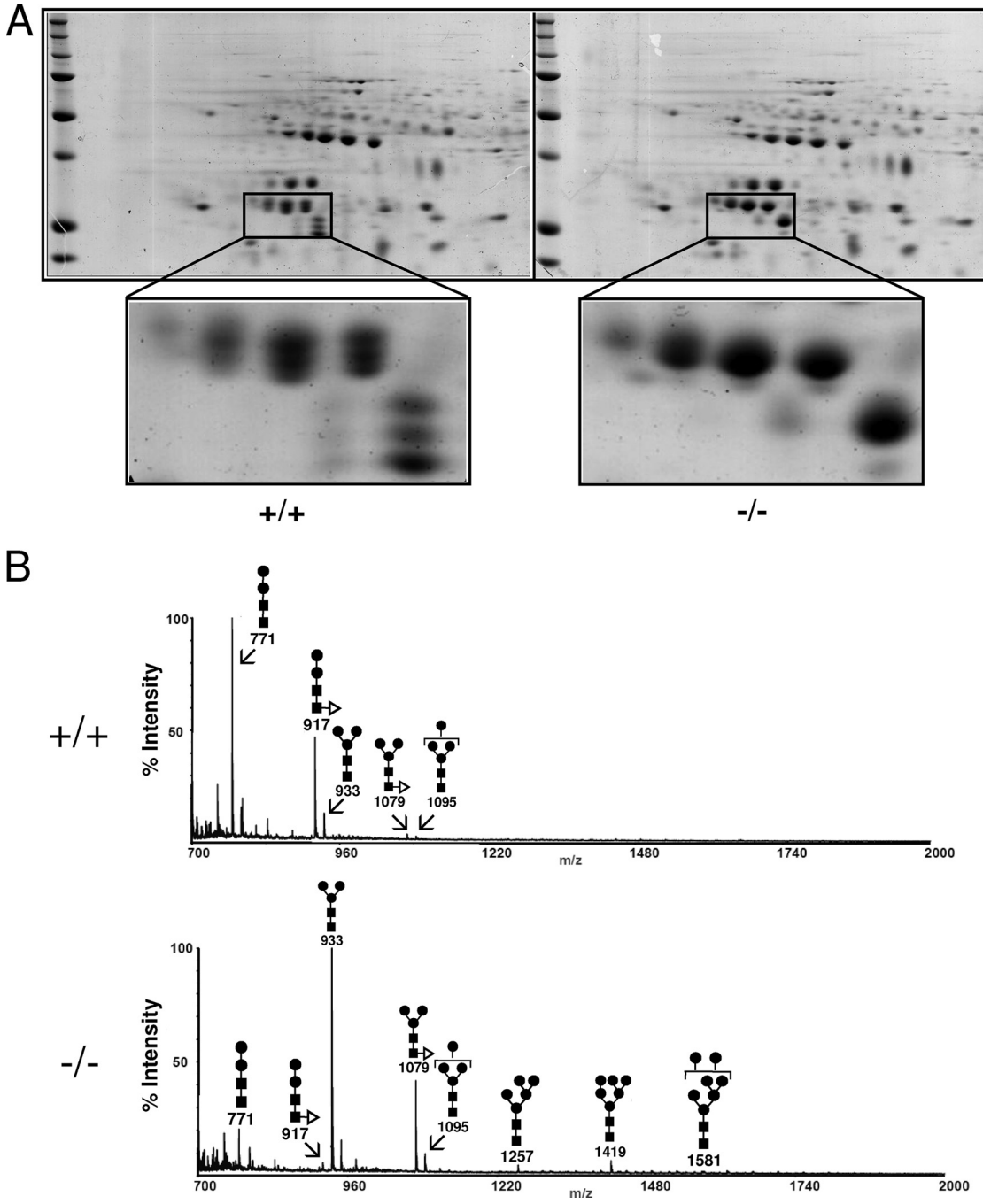

FIG. 5. Isolation and characterization of N-linked oligosaccharides from mouse liver cathepsin B in a lysosome-enriched fraction (F2). (A) Three hundred micrograms of protein of F2 fractions from wild-type mice (+/+, left panel) and mice with α-mannosidosis (−/−, right panel) was separated by 2-D gel electrophoresis and visualized by Coomassie blue staining. Protein spots representing cathepsin B are drawn to a larger scale. (B) N-linked oligosaccharides from cathepsin B spots were released by in-gel PNGase F treatment, pooled, and analyzed by MALDI-TOF mass spectrometry. The symbols for the monosaccharides in the schematic drawing of the oligosaccharide are as follows: black squares represent *N*-acetylglucosamine residues, black circles represent mannose residues, and white triangles represent fucose residues. The numbers below the schematic structures indicate the detected masses of the appropriate oligosaccharides.

perglycosylation can be partially normalized in vivo by ERT with rhLAMAN in mouse and in vitro by incubating a fraction of lysosomal proteins from mice with α-mannosidosis with rhLAMAN. Our results indicate that the lysosomal oligosaccharide trimming on native lysosomal proteins is a common hallmark of lysosomal proteins and that α-mannosidase deficiency results in a general hyperglycosylation of lysosomal proteins. The ERT-mediated correction of the hyperglycosylation phenotype in mice with α-mannosidosis was demonstrated solely for liver. However, correction of the brain defect might

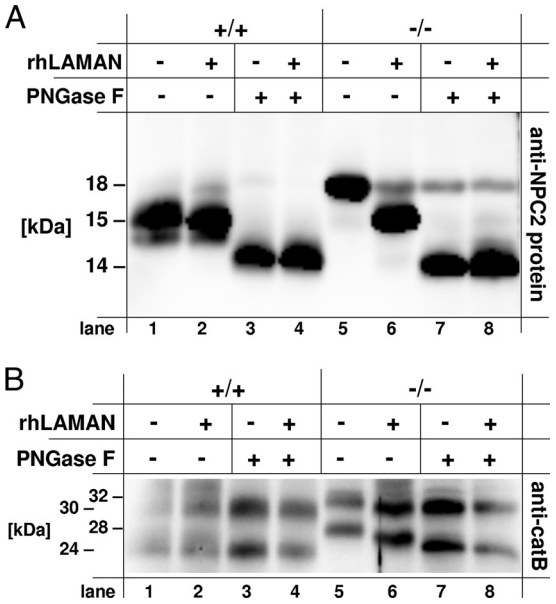

FIG. 6. In vitro normalization of hyperglycosylated lysosomal proteins by rhLAMAN. Thirty micrograms of protein of F2 fractions from wild-type mice (+/+) and mice with α-mannosidosis (−/−) was treated with (+) or without (−) rhLAMAN and subsequently treated in the absence (−) or presence (+) of PNGase F. Finally, the samples were separated by SDS-PAGE and analyzed by immunoblotting using an anti-NPC2 protein antibody (A) and an anti-cathepsin B antibody (B).

be dependent on high-dose ERT (5) or on alternative therapy approaches that lead to enzyme delivery across the blood-brain barrier like bone marrow transplantation in the α-mannosidosis feline model (56) or adeno-associated virus-mediated gene transfer in mice with mucopolysaccharidosis VII (MPS VII) (43) and MPS II (37).

The analysis of cathepsin B-derived oligosaccharides in mice with α-mannosidosis revealed that Man3GlcNAc2 and its fucosylated derivative are mainly occurring on native cathepsin B instead of Man2GlcNAc2 and the fucosylated Man2GlcNAc2 form as seen in control mice. The latter findings with mice are in line with results from rat liver cathepsin B, where 86% of the N-linked oligosaccharides are unfucosylated Man2GlcNAc2, 11% display the fucosylated derivative, and only 3% are Man3GlcNAc2 chains (51). The predominant occurrence of Man3GlcNAc2 oligosaccharides on native cathepsin B in mice with α-mannosidosis suggests a preset order of cleavage with the α1,3-linkage by LAMAN prior to the α1,6-linkage catalyzed by the core-specific α1,6-mannosidase (MAN2B2). Furthermore, it had been demonstrated before that during N-glycan degradation MAN2B2 is dependent on the release of the oligosaccharide from the asparaginyl residue by the activity of the glycosylasparaginase and chitobiase (36). Taken together, we suggest a model for LAMAN function (Fig. 7) in which—besides its known function in the degradation of released oligosaccharides—LAMAN also processes N-glycans on

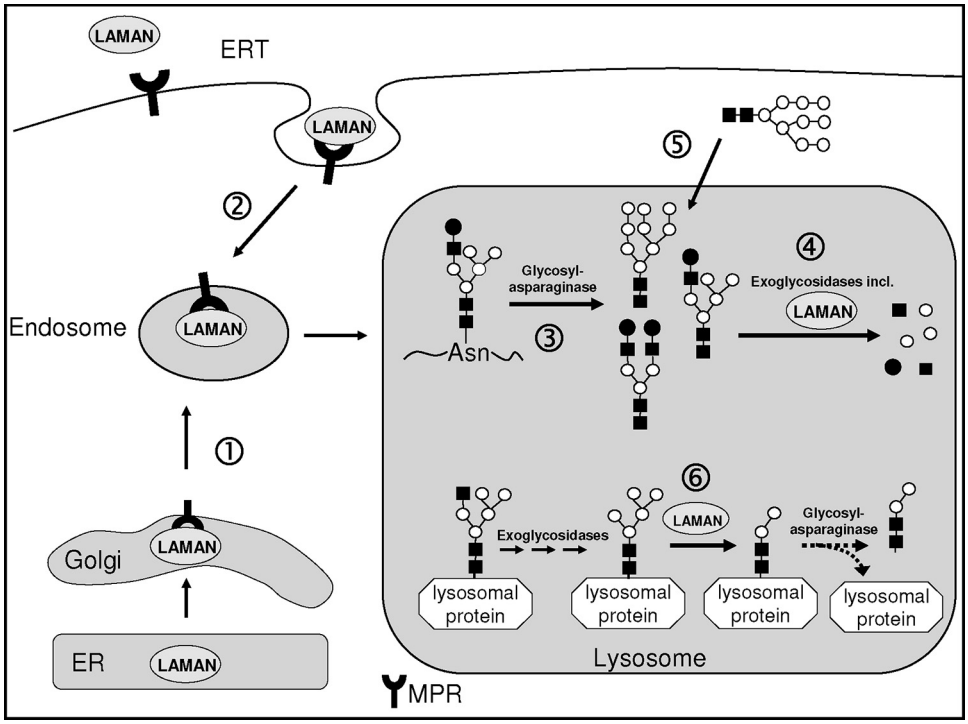

FIG. 7. Schematic diagram of the lysosomal transport of LAMAN and its function inside the lysosome. (1) After synthesis in the endoplasmic reticulum (ER), endogenous mannose 6-phosphate-containing LAMAN is recognized in the Golgi compartment by the mannose 6-phosphate receptor and is delivered to the endosomal/lysosomal compartment. Missorted LAMAN or recombinant LAMAN injected for ERT is recaptured by plasma membrane mannose 6-phosphate receptor (2). During lysosomal degradation of glycoproteins (3), oligosaccharides are released from the asparaginyl residue of the polypeptide and are subsequently degraded by lysosomal exoglycosidases including LAMAN (4). Furthermore, free oligosaccharides (5) are imported from the cytosol by a so-far-unknown mechanism for lysosomal degradation. Besides this well-known catabolic function of LAMAN, our findings demonstrate that LAMAN is involved in the trimming of N-glycans on native lysosomal proteins (6), so that LAMAN deficiency leads to a hypermannosylation of lysosomal proteins.

native lysosomal proteins to the minimum Man2GlcNAc2 form. However, further processing of the N-glycan by MAN2B2 would imply the release of the oligosaccharide from the polypeptide by the glycosylasparaginase.

We also observed microheterogeneity, since high-mannose-type glycans were detected in small amounts in cathepsin B from mice with α-mannosidosis. Consideration of the mannose 6-phosphate-dependent transport of cathepsin B for lysosomal sorting would postulate the presence of at least one high-mannose-type or hybrid-type oligosaccharide and thus a much higher yield of high-mannose oligosaccharides in α-mannosidase-deficient mice. However, mouse cathepsin B possesses three potential N-glycosylation sites, of which one is located in the N-terminal part that is removed upon activation as demonstrated for cathepsin B from rat liver and porcine spleen (49, 50). The N-linked oligosaccharide of the proregion is considered to be phosphorylated and thus responsible for lysosomal transport (50). The remaining two N-glycosylation sites are obviously used in the two-chain form, since we observed three different forms of cathepsin B (Fig. 5). The low-molecular-weight form of cathepsin B is supposed to carry at least a single and thereby undetected *N*-acetylglucosamine, since total deglycosylation would result in a shift in the isoelectric point of the protein due to desamidation of the asparagyl residue.

An increase in the apparent molecular weight of single lysosomal proteins had been described in mouse models for lysosomal storage diseases, e.g., recently for cathepsin D in a mucolipidosis II model (18) and interestingly also for NPC2 protein in the NPC1 protein model, where it was shown to be hyperglycosylation (10). In the latter instance it was discussed as being the result of a trafficking/processing defect. Furthermore, the Acp5-lysosomal acid phosphatase double-knockout model also showed an increased molecular weight for cathepsin D in various tissues like brain, kidney, and spleen (A. Suter and P. Saftig, personal communication). These observations in other LSD mouse models are most likely due to secondary inhibitions of lysosomal exoglycosidases like α-mannosidase, α-fucosidase, or α-sialidase resulting in prolonged N-linked oligosaccharides on lysosomal proteins. Such a secondary inhibition of lysosomal hydrolases would also explain the observation of secondary storage material like gangliosides and cholesterol, which is a common hallmark of LSD as observed in MPSs (for a review, see reference 57).

In contrast, we could demonstrate by detailed mass spectrometry analyses of cathepsin B N-linked oligosaccharides derived from control mice and mice with α-mannosidosis that specifically elongated oligosaccharides with terminal mannosyl residues (up to the Man7GlcNAc2 form) are enriched in mice with α-mannosidosis, and most remarkably, we were able to correct the hypermannosylation in vitro and in vivo, suggesting that the hypermannosylation is a primary and direct effect of α-mannosidase deficiency. Such primary defects of the modification of oligosaccharide had been described 25 years ago indirectly in lectin binding studies for complex-type oligosaccharide chains of glycoproteins derived from galactosialidosis patients showing hypersialylated glycoproteins (34, 48) that were removed by ERT with lysosomal α-sialidase or protective protein/cathepsin A in fibroblasts from galactosialidosis patients. As another example, it was shown that the action of exoglycosidases is required to mature the lysosomal hydrolase glucocerebrosidase (53). These findings prompted Elizabeth Neufeld to expand the term "carbohydrate trimming" on the lysosomal compartment (33). The biochemical consequences that arise from the hyperglycosylation of lysosomal glycoproteins are not predictable since, e.g., glucocerebrosidase shows—regardless of its glycosylation status—no effect on relative catalytic activity (53). On the other hand, it was demonstrated for recombinant human NPC2 protein that the diglycosylated NPC2 protein exhibited significantly lower cholesterol transfer rates (three- to fourfold) than the monoglycosylated NPC2 variant, most likely due to charge repulsions between the oligosaccharides and anionic groups of the phospholipids (27). Comparably, it was shown that the deglycosylation of the lysosomal β-glucosidase as well as TPP1 leads to a complete loss of enzyme activity (20, 35). Hyperglycosylation of N-linked oligosaccharides due to an impaired trimming had been described for Golgi α-mannosidase II deficiency, also called HEMPAS (*h*ereditary *e*rythroblastic *m*ultinuclearity with a *p*ositive *a*cidified *s*erum lysis test), leading to a reduced ability to form complex-type oligosaccharides (11). The unpredictability of the glycosylation impact on the function of glycoproteins has to be ascribed to the different tasks and functions in terms of its influence on the conformational properties and solubility of glycoproteins and its function in control of half-life by conferring resistance to denaturation and proteolysis as well as its effect on enzymatic activities and protein-substrate interactions (22, 42, 54).

In summary, we demonstrate the existence of hyperglycosylated lysosomal proteins with terminal mannosyl residues in mice lacking LAMAN, suggesting a direct role of lysosomal exoglycosidases in the trimming of oligosaccharides on native lysosomal proteins. Furthermore, the hyperglycosylation of lysosomal proteins in mice with α-mannosidosis could be partially reversed in vivo by ERT using rhLAMAN and in vitro by incubation with rhLAMAN.

ACKNOWLEDGMENTS

We thank Nicole Eiselt and Klaus Neifer for excellent technical assistance and Kurt von Figura for critical reading of the manuscript.

This work was supported by the HUE-MAN consortium (European Commission FP VI contract LHSM-CT-2006-018692) as well as by the Centre National de la Recherche (Unité Mixte de Recherche CNRS/USTL 8576) and the Ministère de la Recherche et de l'Enseignement Supérieur. The Mass Spectrometry facility in Lille was funded by the European Community (FEDER), the Région Nord-Pas de Calais (France), and the Université des Sciences et Technologies de Lille.

REFERENCES

1. **Abraham, D., W. F. Blakemore, R. D. Jolly, R. Sidebotham, and B. Winchester.** 1983. The catabolism of mammalian glycoproteins. Comparison of the storage products in bovine, feline and human mannosidosis. Biochem. J. **215:**573–579.
2. **Aronson, N. N., Jr., and M. J. Kuranda.** 1989. Lysosomal degradation of Asn-linked glycoproteins. FASEB J. **3:**2615–2622.
3. **Auclair, D., and J. J. Hopwood.** 2007. Morphopathological features in tissues of alpha-mannosidosis guinea pigs at different gestational ages. Neuropathol. Appl. Neurobiol. **33:**572–585.
4. **Bennet, J. K., P. P. Dembure, and L. J. Elsas.** 1995. Clinical and biochemical analysis of two families with type I and type II mannosidosis. Am. J. Med. Genet. **55:**21–26.
5. **Blanz, J., S. Stroobants, R. Lullmann-Rauch, W. Morelle, M. Ludemann, R. D'Hooge, H. Reuterwall, J. C. Michalski, J. Fogh, C. Andersson, and P. Saftig.** 2008. Reversal of peripheral and central neural storage and ataxia after recombinant enzyme replacement therapy in alpha-mannosidosis mice. Hum. Mol. Genet. **17:**3437–3445.
6. **Borland, N. A., I. V. Jerrett, and D. H. Embury.** 1984. Mannosidosis in aborted and stillborn Galloway calves. Vet. Rec. **114:**403–404.

7. **Bresciani, R., and K. Von Figura.** 1996. Dephosphorylation of the mannose-6-phosphate recognition marker is localized in later compartments of the endocytic route. Identification of purple acid phosphatase (uteroferrin) as the candidate phosphatase. Eur. J. Biochem. **238:**669–674.
8. **Burditt, L. J., K. Chotai, S. Hirani, P. G. Nugent, B. G. Winchester, and W. F. Blakemore.** 1980. Biochemical studies on a case of feline mannosidosis. Biochem. J. **189:**467–473.
9. **Chantret, I., and S. E. Moore.** 2008. Free oligosaccharide regulation during mammalian protein N-glycosylation. Glycobiology **18:**210–224.
10. **Chen, F. W., R. E. Gordon, and Y. A. Ioannou.** 2005. NPC1 late endosomes contain elevated levels of non-esterified (′free′) fatty acids and an abnormally glycosylated form of the NPC2 protein. Biochem. J. **390:**549–561.
11. **Chui, D., M. Oh-Eda, Y. F. Liao, K. Panneerselvam, A. Lal, K. W. Marek, H. H. Freeze, K. W. Moremen, M. N. Fukuda, and J. D. Marth.** 1997. Alpha-mannosidase-II deficiency results in dyserythropoiesis and unveils an alternate pathway in oligosaccharide biosynthesis. Cell **90:**157–167.
12. **Crawley, A. C., M. Z. Jones, L. E. Bonning, J. W. Finnie, and J. J. Hopwood.** 1999. Alpha-mannosidosis in the guinea pig: a new animal model for lysosomal storage disorders. Pediatr. Res. **46:**501–509.
13. **Crawley, A. C., B. King, T. Berg, P. J. Meikle, and J. J. Hopwood.** 2006. Enzyme replacement therapy in alpha-mannosidosis guinea-pigs. Mol. Genet. Metab. **89:**48–57.
14. **Daniel, P. F., B. Winchester, and C. D. Warren.** 1994. Mammalian alpha-mannosidases—multiple forms but a common purpose? Glycobiology **4:**551–566.
15. **de Duve, C., B. Pressman, R. Gianetto, R. Wattiaux, and F. Appelmans.** 1955. Tissue fraction studies. 6. Intracellular distribution patterns of enzymes in rat liver tissue. Biochem. J. **60:**604–617.
16. **Einstein, R., and C. A. Gabel.** 1991. Cell- and ligand-specific dephosphorylation of acid hydrolases: evidence that the mannose 6-phosphatase is controlled by compartmentalization. J. Cell Biol. **112:**81–94.
17. **Gabel, C. A., and S. A. Foster.** 1986. Mannose 6-phosphate receptor-mediated endocytosis of acid hydrolases: internalization of beta-glucuronidase is accompanied by a limited dephosphorylation. J. Cell Biol. **103:**1817–1827.
18. **Gelfman, C. M., P. Vogel, T. M. Issa, C. A. Turner, W. S. Lee, S. Kornfeld, and D. S. Rice.** 2007. Mice lacking alpha/beta subunits of GlcNAc-1-phosphotransferase exhibit growth retardation, retinal degeneration, and secretory cell lesions. Invest. Ophthalmol. Vis. Sci. **48:**5221–5228.
19. **Golabek, A. A., and E. Kida.** 2006. Tripeptidyl-peptidase I in health and disease. Biol. Chem. **387:**1091–1099.
20. **Grace, M. E., and G. A. Grabowski.** 1990. Human acid beta-glucosidase: glycosylation is required for catalytic activity. Biochem. Biophys. Res. Commun. **168:**771–777.
21. **Haeuw, J. F., T. Grard, C. Alonso, G. Strecker, and J. C. Michalski.** 1994. The core-specific lysosomal alpha(1-6)-mannosidase activity depends on aspartamidohydrolase activity. Biochem. J. **297:**463–466.
22. **Helenius, A., and M. Aebi.** 2001. Intracellular functions of N-linked glycans. Science **291:**2364–2369.
23. **Hirsch, C., D. Blom, and H. L. Ploegh.** 2003. A role for N-glycanase in the cytosolic turnover of glycoproteins. EMBO J. **22:**1036–1046.
24. **Hocking, J. D., R. D. Jolly, and R. D. Batt.** 1972. Deficiency of alpha-mannosidase in Angus cattle. An inherited lysosomal storage disease. Biochem. J. **128:**69–78.
25. **Kollmann, K., M. Damme, F. Deuschl, J. Kahle, R. D'Hooge, R. Lullmann-Rauch, and T. Lubke.** 2009. Molecular characterization and gene disruption of mouse lysosomal putative serine carboxypeptidase 1. FEBS J. **276:**1356–1369.
26. **Kollmann, K., K. E. Mutenda, M. Balleininger, E. Eckermann, K. von Figura, B. Schmidt, and T. Lubke.** 2005. Identification of novel lysosomal matrix proteins by proteome analysis. Proteomics **5:**3966–3978.
27. **Liou, H. L., S. S. Dixit, S. Xu, G. S. Tint, A. M. Stock, and P. Lobel.** 2006. NPC2, the protein deficient in Niemann-Pick C2 disease, consists of multiple glycoforms that bind a variety of sterols. J. Biol. Chem. **281:**36710–36723.
28. **Mach, L.** 2002. Biosynthesis of lysosomal proteinases in health and disease. Biol. Chem. **383:**751–756.
29. **Malm, D., and O. Nilssen.** 2008. Alpha-mannosidosis. Orphanet J. Rare Dis. **3:**21.
30. **Michalski, J. C., J. F. Haeuw, J. M. Wieruszeski, J. Montreuil, and G. Strecker.** 1990. In vitro hydrolysis of oligomannosyl oligosaccharides by the lysosomal alpha-D-mannosidases. Eur. J. Biochem. **189:**369–379.
31. **Michalski, J. C., and A. Klein.** 1999. Glycoprotein lysosomal storage disorders: alpha- and beta-mannosidosis, fucosidosis and alpha-N-acetylgalactosaminidase deficiency. Biochim. Biophys. Acta **1455:**69–84.
32. **Moore, S. E.** 1999. Oligosaccharide transport: pumping waste from the ER into lysosomes. Trends Cell Biol. **9:**441–446.
33. **Neufeld, E. F.** 1991. Lysosomal storage diseases. Annu. Rev. Biochem. **60:**257–280.
34. **Oheda, Y., M. Kotani, M. Murata, H. Sakuraba, Y. Kadota, Y. Tatano, J. Kuwahara, and K. Itoh.** 2006. Elimination of abnormal sialylglycoproteins in fibroblasts with sialidosis and galactosialidosis by normal gene transfer and enzyme replacement. Glycobiology **16:**271–280.
35. **Pal, A., R. Kraetzner, T. Gruene, M. Grapp, K. Schreiber, M. Gronborg, H. Urlaub, S. Becker, A. R. Asif, J. Gartner, G. M. Sheldrick, and R. Steinfeld.** 2009. Structure of tripeptidyl-peptidase I provides insight into the molecular basis of late infantile neuronal ceroid lipofuscinosis. J. Biol. Chem. **284:**3976–3984.
36. **Park, C., L. Meng, L. H. Stanton, R. E. Collins, S. W. Mast, X. Yi, H. Strachan, and K. W. Moremen.** 2005. Characterization of a human core-specific lysosomal {alpha}1,6-mannosidase involved in N-glycan catabolism. J. Biol. Chem. **280:**37204–37216.
37. **Polito, V. A., and M. P. Cosma.** 2009. IDS crossing of the blood-brain barrier corrects CNS defects in MPSII mice. Am. J. Hum. Genet. **85:**296–301.
38. **Robinson, A. J., A. C. Crawley, D. Auclair, P. F. Weston, C. Hirte, K. M. Hemsley, and J. J. Hopwood.** 2008. Behavioural characterisation of the alpha-mannosidosis guinea pig. Behav. Brain Res. **186:**176–184.
39. **Roces, D. P., R. Lullmann-Rauch, J. Peng, C. Balducci, C. Andersson, O. Tollersrud, J. Fogh, A. Orlacchio, T. Beccari, P. Saftig, and K. von Figura.** 2004. Efficacy of enzyme replacement therapy in alpha-mannosidosis mice: a preclinical animal study. Hum. Mol. Genet. **13:**1979–1988.
40. **Saftig, P.** 2005. Lysosomes. Landes Bioscience/Eurekah.com, New York, NY.
41. **Saint-Pol, A., P. Codogno, and S. E. Moore.** 1999. Cytosol-to-lysosome transport of free polymannose-type oligosaccharides. Kinetic and specificity studies using rat liver lysosomes. J. Biol. Chem. **274:**13547–13555.
42. **Sears, P., and C. H. Wong.** 1998. Enzyme action in glycoprotein synthesis. Cell. Mol. Life Sci. **54:**223–252.
43. **Sferra, T. J., K. Backstrom, C. Wang, R. Rennard, M. Miller, and Y. Hu.** 2004. Widespread correction of lysosomal storage following intrahepatic injection of a recombinant adeno-associated virus in the adult MPS VII mouse. Mol. Ther. **10:**478–491.
44. **Sleat, D. E., I. Sohar, H. Lackland, J. Majercak, and P. Lobel.** 1996. Rat brain contains high levels of mannose-6-phosphorylated glycoproteins including lysosomal enzymes and palmitoyl-protein thioesterase, an enzyme implicated in infantile neuronal lipofuscinosis. J. Biol. Chem. **271:**19191–19198.
45. **Spiro, R. G.** 2004. Role of N-linked polymannose oligosaccharides in targeting glycoproteins for endoplasmic reticulum-associated degradation. Cell. Mol. Life Sci. **61:**1025–1041.
46. **Stinchi, S., R. Lullmann-Rauch, D. Hartmann, R. Coenen, T. Beccari, A. Orlacchio, K. von Figura, and P. Saftig.** 1999. Targeted disruption of the lysosomal alpha-mannosidase gene results in mice resembling a mild form of human alpha-mannosidosis. Hum. Mol. Genet. **8:**1365–1372.
47. **Sun, P., D. E. Sleat, M. Lecocq, A. R. Hayman, M. Jadot, and P. Lobel.** 2008. Acid phosphatase 5 is responsible for removing the mannose 6-phosphate recognition marker from lysosomal proteins. Proc. Natl. Acad. Sci. U. S. A. **105:**16590–16595.
48. **Swallow, D. M., L. F. West, and A. Van Elsen.** 1984. The role of lysosomal sialidase and beta-galactosidase in processing the complex carbohydrate chains on lysosomal enzymes and possibly other glycoproteins. Ann. Hum. Genet. **48:**215–221.
49. **Takahashi, T., P. G. Schmidt, and J. Tang.** 1984. Novel carbohydrate structures of cathepsin B from porcine spleen. J. Biol. Chem. **259:**6059–6062.
50. **Tanaka, Y., R. Tanaka, T. Kawabata, Y. Noguchi, and M. Himeno.** 2000. Lysosomal cysteine protease, cathepsin B, is targeted to lysosomes by the mannose 6-phosphate-independent pathway in rat hepatocytes: site-specific phosphorylation in oligosaccharides of the proregion. J. Biochem. **128:**39–48.
51. **Taniguchi, T., T. Mizuochi, T. Towatari, N. Katunuma, and A. Kobata.** 1985. Structural studies on the carbohydrate moieties of rat liver cathepsins B and H. J. Biochem. **97:**973–976.
52. **Turk, V., B. Turk, and D. Turk.** 2001. Lysosomal cysteine proteases: facts and opportunities. EMBO J. **20:**4629–4633.
53. **Van Weely, S., J. M. Aerts, M. B. Van Leeuwen, J. C. Heikoop, W. E. Donker-Koopman, J. A. Barranger, J. M. Tager, and A. W. Schram.** 1990. Function of oligosaccharide modification in glucocerebrosidase, a membrane-associated lysosomal hydrolase. Eur. J. Biochem. **191:**669–677.
54. **Varki, A.** 1993. Biological roles of oligosaccharides: all of the theories are correct. Glycobiology **3:**97–130.
55. **Walkley, S. U., W. F. Blakemore, and D. P. Purpura.** 1981. Alterations in neuron morphology in feline mannosidosis. A Golgi study. Acta Neuropathol. **53:**75–79.
56. **Walkley, S. U., M. A. Thrall, K. Dobrenis, M. Huang, P. A. March, D. A. Siegel, and S. Wurzelmann.** 1994. Bone marrow transplantation corrects the enzyme defect in neurons of the central nervous system in a lysosomal storage disease. Proc. Natl. Acad. Sci. U. S. A. **91:**2970–2974.
57. **Walkley, S. U., and M. T. Vanier.** 2009. Secondary lipid accumulation in lysosomal disease. Biochim. Biophys. Acta **1793:**726–736.
58. **Wattiaux, R., M. Wibo, and P. Baudhuin.** 1963. Effect of the injection of Triton WR 1339 on the hepatic lysosomes of the rat. Arch. Int. Physiol. Biochim. **71:**140–142. (In French.)
59. **Willenborg, M., C. K. Schmidt, P. Braun, J. Landgrebe, K. von Figura, P. Saftig, and E. L. Eskelinen.** 2005. Mannose 6-phosphate receptors, Niemann-Pick C2 protein, and lysosomal cholesterol accumulation. J. Lipid Res. **46:**2559–2569.
60. **Winchester, B.** 1984. Role of alpha-D-mannosidases in the biosynthesis and catabolism of glycoproteins. Biochem. Soc. Trans. **12:**522–524.
61. **Winchester, B.** 2005. Lysosomal metabolism of glycoproteins. Glycobiology **15:**1R–15R.